JACS
JOURNAL OF THE AMERICAN CHEMICAL SOCIETY

COMMUNICATION

pubs.acs.org/JACS

High-Field Dynamic Nuclear Polarization with High-Spin Transition Metal Ions

Björn Corzilius,[†] Albert A. Smith,[†] Alexander B. Barnes,[†] Claudio Luchinat,[‡] Ivano Bertini,[‡] and Robert G. Griffin*[,†]

[†]Department of Chemistry and Francis Bitter Magnet Laboratory, Massachusetts Institute of Technology, 77 Massachusetts Avenue, Cambridge, Massachusetts 02139, United States

[‡]Magnetic Resonance Center and Department of Chemistry, University of Florence, Via L. Sacconi 6, 50019 Sesto Fiorentino (FI), Italy

Supporting Information

ABSTRACT: We report the dynamic nuclear polarization of ^{1}H spins in magic-angle-spinning spectra recorded at 5 T and 84 K via the solid effect using Mn^{2+} and Gd^{3+} complexes as polarizing agents. We show that the magnitude of the enhancements can be directly related to the effective line width of the central ($m_S = -^1/_2 \rightarrow +^1/_2$) EPR transition. Using a Gd^{3+} complex with a narrow central transition EPR line width of 29 MHz, we observed a maximum enhancement of ~13, which is comparable to previous results on the narrow-line-width trityl radical.

Applications of magic-angle-spinning NMR spectroscopy (MAS NMR) are often limited by the low Boltzmann polarization of nuclear spins and therefore the low inherent sensitivity. Thus, in samples such as large biomolecules or compounds with a low abundance of magnetic nuclei, the experimental acquisition time can be prohibitively long. The same is true even when uniformly ^{13}C/^{15}N-labeled samples are employed and multidimensional techniques are required to perform assignments and measure ^{13}C−^{15}N and ^{13}C−^{13}C distances and torsion angles.[1−4] In such cases, high-frequency dynamic nuclear polarization (DNP) can be used to significantly boost the sensitivity of MAS NMR by transferring the relatively large polarization of electron spins to the nuclei.[5−10] Accordingly, DNP has been successfully applied to the investigation of functional membrane proteins in their native lipid environments[11,12] and amyloid fibrils[13−16] without compromising the spectral resolution.[17] These experiments would not be feasible in a reasonable amount of time with conventional MAS NMR.

The polarizing agents used in contemporary DNP experiments have primarily been persistent $g \approx 2$ organic radicals [e.g., trityl, 1,3-bis(diphenylene)-2-phenylallyl (BDPA), and nitroxide-based mono- and biradicals].[18−20] In principle, however, paramagnetic metal ions can also be used as a source of polarization, and they offer at least two potential advantages. First, many metalloproteins contain paramagnetic metals or can be doped with a paramagnetic substitute, thus providing an intrinsic source of polarization that could lead to efficient enhancement of protein resonances. Second, they offer the possibility of locally polarizing the nuclei adjacent to the metal and thus could yield site-specific structural details for the active sites of metalloproteins. In addition, this local character of the polarization could provide important details about the DNP process. Besides that, many inorganic samples often contain or can be doped with paramagnetic metal ions. This opens the possibility of applying DNP to a variety of materials science-related problems. For these reasons, we initiated investigations of DNP enhancements with high-spin transition-metal ions, and we report the initial results for Gd^{3+} and Mn^{2+} in this communication.

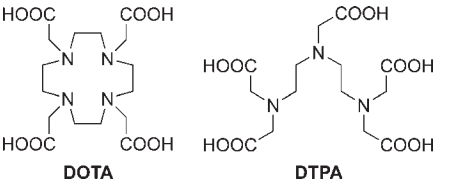

Figure 1. Chemical structures of the (protonated) octadentate chelating ligands DOTA and DTPA.

The two metals were used in the form of complexes with the octadentate chelating ligands 1,4,7,10-tetraazacyclododecane-1,4,7,10-tetraacetic acid (DOTA) and diethylenetriaminepentaacetic acid (DTPA) (Figure 1). These ligands form extremely stable complexes and are used as magnetic resonance imaging contrast agents in clinical applications. Furthermore, Gd^{3+} complexes with DOTA and DTPA exhibit significantly different electric field gradients at the metal site,[21] allowing us to investigate the influence of the magnitude of the zero-field splitting (ZFS) on the efficiency of the DNP process. Experimental details about both the DNP/NMR and EPR experiments are available in the Supporting Information.

The DNP mechanism that governs the polarization transfer in the compounds used in this study is the solid effect (SE).[22] This is a two-spin process in which microwave irradiation at $\omega_{mw} = \omega_{0S} \pm \omega_{0I}$ (where ω_{0S} and ω_{0I} are the electron and nuclear Larmor frequencies, respectively) excites forbidden electron−nucleus transitions that become partially allowed through mixing of adjacent states. The Hamiltonian relevant to this system is

$$\hat{H} = \omega_{0S}\hat{S}_Z - \omega_{0I}\hat{I}_Z + A\hat{S}_Z\hat{I}_Z + C\hat{S}_Z\hat{I}_+ + C^*\hat{S}_Z\hat{I}_-$$

where A is the secular hyperfine coupling constant, $C = -^3/_2(\gamma_S\gamma_I/r^3)$ sin θ cos θ $e^{-i\varphi}$ is the usual term in the van Vleck form of the electron−nuclear dipole Hamiltonian, and $\hat{S}$ and $\hat{I}$ are spin operators for electrons and nuclei, respectively.[23] Double- or zero-quantum

Received: December 4, 2010
Published: March 29, 2011

dx.doi.org/10.1021/ja1109002 | J. Am. Chem. Soc. 2011, 133, 5648–5651

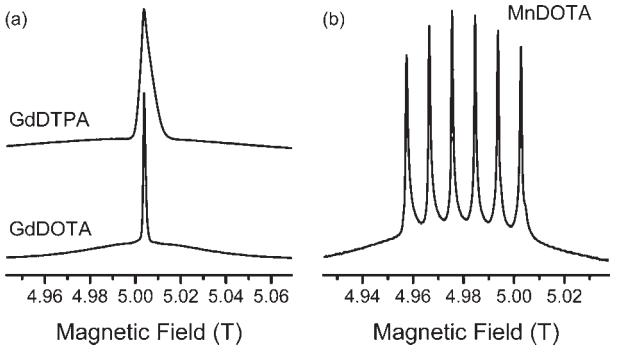

Figure 2. EPR spectra of the complexes under investigation, recorded at 139.5 GHz using a Hahn echo sequence. The solution [1 mM in 60:40 (v/v) glycerol/H_2O] was contained in a 0.5 mm o.d. quartz capillary at a temperature of 20 K.

transitions that are partially allowed as a result of state mixing by the $\hat{S}_Z\hat{I}_\pm$ terms are excited at ω_{mw} and transfer polarization from the electron spins to the nuclear spins. The transition probabilities scale with the magnetic field as ω_{0I}^{-2}.[24,25] A requirement for a large SE enhancement (ε) is that both the homogeneous (δ) and inhomogeneous (Δ) EPR linewidths of the paramagnetic center be smaller than ω_{0I} of the nucleus to be polarized (i.e., $\delta,\Delta \ll 2\omega_{0I}$). When this criterion is not satisfied, the zero- and double-quantum transitions broaden or overlap, leading to cancellation of positive and negative enhancements. The remaining net enhancement is due to a differential solid effect (DSE). In addition, large γB_1 values are known to increase SE enhancements. For example, in experiments to be reported elsewhere,[26] $\varepsilon \approx 100$ was observed using trityl as a polarizing agent at the high microwave field strengths available in a microwave resonator. Despite these limitations, significant enhancements of ~15 can be observed using even moderate γB_1 values and B_0 = 5 T.[25]

EPR spectra (140 GHz) of all three complexes in the form of glassy solutions are shown in Figure 2. As can be seen in the case of Gd^{3+} ($S = {}^7/_2$), each EPR signal consists of a narrow resonance arising from the central ($m_S = -{}^1/_2 \rightarrow +{}^1/_2$) transition and a broad resonance resulting from single-quantum transitions (${}^7/_2 \rightarrow {}^5/_2 \rightarrow {}^3/_2$, etc.) that are broadened by the ZFS. Although neither ligand significantly alters the g value of Gd^{3+} (g = 1.9918), the line widths of the central EPR lines differ by more than a factor of 5 (29 MHz full width at half maximum (fwhm) for GdDOTA and 150 MHz for GdDTPA). This difference is due to the significant difference in the ZFS constants (D = 0.57 GHz, E = 0 for GdDOTA; D = 1.44 GHz, E = 0.39 GHz for GdDTPA).[21] Though the central transition is not affected by the ZFS to first order, residual second-order effects that scale with D^2/ω_0 lead to nonvanishing coupling effects that govern the line width of the central transition.[27] Therefore, other broadening mechanisms such as g strain, hyperfine coupling to ^{155}Gd and ^{157}Gd (both of which are present with a natural abundance of ~15%) and ^{14}N, and homogeneous broadening can be considered as small relative to the second-order ZFS for both Gd^{3+} complexes. Although this line-broadening mechanism is not present in $S = {}^1/_2$ systems, the SE experiments reported to date using carbon-centered radicals in aqueous solutions have utilized a minimum line width of 55 MHz observed with trityl,[28] which is still significantly broader than the GdDOTA line.

The EPR spectrum of MnDOTA shows the typical sextet pattern centered at g = 2.0014 due to hyperfine coupling to ^{55}Mn ($I = {}^5/_2$) with a hyperfine coupling constant of A = 254 MHz. Again, only the central transition of the high-spin ($S = {}^5/_2$) system yields narrow

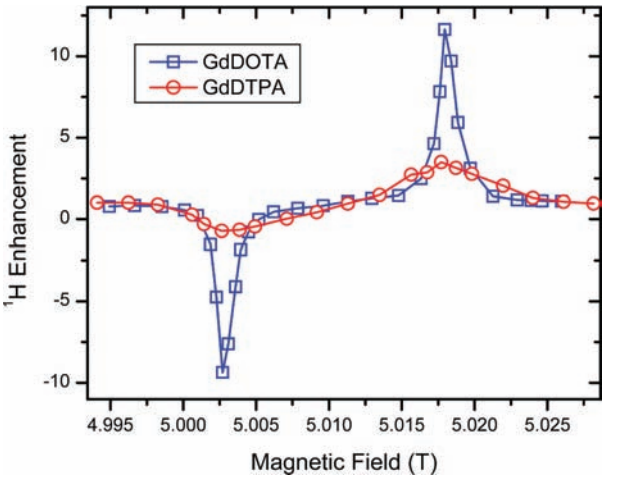

Figure 3. Field-dependent DNP enhancement profiles of GdDOTA and GdDTPA recorded at 84 K with a microwave frequency of 139.65 GHz, a microwave power of 6 W, and an MAS frequency of 5 kHz. Data points were obtained by directly detecting the ^1H polarization via a Bloch decay.

EPR lines, whereas the higher spin transitions are broadened by the ZFS and contribute to the spectrum as a broad component visible in the spectrum. The fwhm of each central line is ~25 MHz. Despite the narrow line width, we expect a reduced enhancement because the $S = {}^1/_2$ transition is dispersed by the $m_S = -{}^1/_2 \rightarrow +{}^1/_2$ nuclear hyperfine coupling.

In a high-spin system ($S = {}^5/_2$ or ${}^7/_2$), the selective polarization of the $m_S = -{}^1/_2 \rightarrow +{}^1/_2$ transition is less than for $S = {}^1/_2$. For the $S = {}^7/_2$ Gd^{3+} system, the relative polarization (population difference in the $m_S = -{}^1/_2 \rightarrow +{}^1/_2$ subspace divided by the total population of all m_S states) is one-fourth of that of an $S = {}^1/_2$ system, and for Mn^{2+} ($S = {}^5/_2$), it is one-third. However, in the case of Mn^{2+}, the selection of only one line of the hyperfine sextet leads to an effective reduction of the selective relative polarization to only ${}^1/_{18}$. For both the Gd^{3+} and Mn^{2+} complexes, a concentration of 10 mM in 60:30:10 (v/v) glycerol-d_8/D_2O/H_2O yielded the maximum enhancements and was chosen for all experiments.

The field-dependent enhancement profiles of the Gd^{3+} compounds (Figure 3) exhibit the shape characteristic of the SE. In the case of GdDOTA, the positive and negative enhancement peaks are well-separated, since the overall EPR line width of the central transition (29 MHz) is much smaller than the ^1H Larmor frequency (213 MHz). In contrast, GdDTPA approaches the condition for DSE because the EPR line width is comparable to the ^1H Larmor frequency (150 vs 213 MHz). The maximum enhancements obtained at 6 W microwave power[29−31] for GdDTPA and GdDOTA were 3.5 and 12.8, respectively. Thus, because of the line width at this field, GdDTPA is not an attractive polarizing agent. A similar Gd^{3+} line width was present in a recent study of polarization transfer in DNP experiments. However, only the decay of the EPR signals, rather than the nuclear polarization, was examined in that study.[32]

In contrast, for GdDOTA, ε = 12.8, which is comparable to the performance of conventional trityl polarizing agents ($\varepsilon \approx 15$). This result is quite surprising since the population difference in the $m_S = -{}^1/_2 \rightarrow +{}^1/_2$ subspace of the high-spin system is only about one-fourth of the polarization found in an $S = {}^1/_2$ system. A possible reason for the relatively good DNP performance might be the 4-fold larger transition moment of the $S = {}^7/_2$ central transition relative to those of low-spin ($S = {}^1/_2$) radical centers,[33] which corresponds to a 16-fold increase in the effective

dx.doi.org/10.1021/ja1109002 |J. Am. Chem. Soc. 2011, 133, 5648–5651

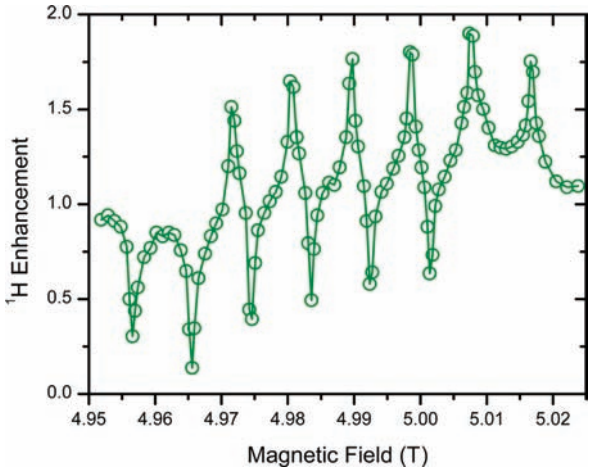

Figure 4. Field-dependent DNP enhancement profiles of MnDOTA recorded at 86 K using a microwave frequency of 139.65 GHz and a microwave power of 5 W. For further details, see Figure 2.

microwave power. However, this neglects the contribution of the higher-m_S transitions to paramagnetic relaxation. Additionally, the complex relationship between electronic relaxation, nuclear relaxation, hyperfine coupling, and double- and zero-quantum transition moments and their respective influence on DNP efficiency remains to be elucidated theoretically and experimentally.

The field-dependent enhancement profile of MnDOTA (Figure 4) has a more complicated structure that reflects the overlap of two hyperfine sextets with amplitudes of opposite sign that are shifted by twice the ^{1}H Larmor frequency with respect to one another. Because of the narrow line width of the SE transitions and the mismatch between the ^{1}H Larmor frequency and the hyperfine coupling (212 vs 254 MHz), all 12 DNP peaks are clearly resolved. However, the maximum enhancement observed at the second outermost peak on the high-field side is only ~1.9 at a microwave power of 5 W. We ascribe this small enhancement to the distribution of the DNP conditions over all six hyperfine lines, which leads to an even smaller fraction ($^1/_{18}$) of spins involved in the DNP process in comparison with the Gd^{3+} case, in which ~70% of the nuclear spins lack a magnetic moment and the hyperfine coupling to the magnetically active nuclei is too small to have a significant impact on the line width. In addition, the lower spin state of Mn^{2+} ($S = {}^5/_2$) and the lower transition moment of the central EPR transition (3 times larger than that for $S = {}^1/_2$) might result in a slightly lower performance than for Gd^{3+}.

To compare the relative performances of the different polarizing agents quantitatively, we evaluated the areas under the field-dependent polarization profiles ($\varepsilon - 1$). We emphasize that the shape and width of the enhancement profile peak are neither influenced by nor similar in line width to the enhanced ^{1}H NMR signal. Rather, they primarily reflect the line width of the EPR central transition; in fact, the field-swept DNP profile can be considered as an EPR spectrum being detected indirectly via the ^{1}H enhancement. Thus, the integral over the DNP peak should allow us to compare the different paramagnetic species independent of the line widths of their EPR central transitions. The intended integration was straightforward in the case of the two Gd^{3+} compounds, since we could integrate over the complete positive enhancement peak. In contrast, the full integration was not possible in the case of the Mn^{2+} complex because of the overlap of the hyperfine lines of the positive and negative DNP peaks. Therefore, we integrated over only the two high-field peaks that were clearly resolved and well-separated from any negative DNP condition and then multiplied the result by 3. The results of this simple analysis are summarized in Table 1. Despite the very different maximum enhancements obtained from the three compounds, the integrated enhancements, which represent excitation of all transitions yielding positive enhancement, are very similar. GdDTPA performed ~30% less efficiently than the corresponding DOTA complex, which might be caused by the onset of the DSE condition. Although there should be little overlap of double- and zero-quantum transitions at the centers of the respective peaks, there should be some cancellation effects, especially closer to the center of the enhancement profile. However, since the use of a monochromatic microwave source did not allow us to utilize this integral enhancement, these results show that the effect of spectral dilution due to ZFS or hyperfine coupling dominates the actual enhancement obtained under experimental DNP conditions. Since the magnitude of the second-order ZFS that broadens the central transition scales inversely as the external magnetic field, these compounds at yet higher fields might potentially outperform organic radicals like trityl, whose EPR resonances are mostly broadened by g anisotropy under these conditions.[28]

Table 1. Experimental DNP Parameters

sample	enhancement	integral enhancement	buildup time (s)
GdDOTA[a]	12.8	0.98	6.6
GdDTPA[a]	3.5	0.70	5.2
MnDOTA[b]	1.9	0.89	5.6

[a] At 6 W microwave power. [b] At 5 W microwave power. For further details, see the text.

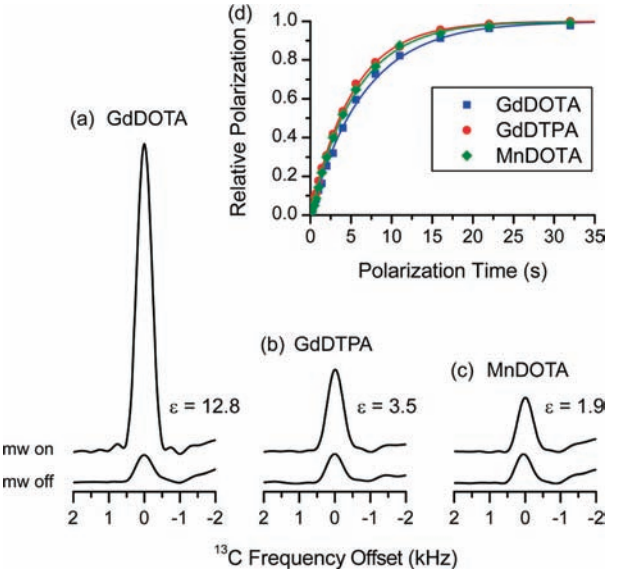

Figure 5. (a–c) Comparison of the microwave-on and -off signals detected after transfer of the ^{1}H polarization to ^{13}C (in 1 M ^{13}C-urea) via cross-polarization. Both Gd^{3+} complexes were measured at 84 K and 6 W microwave power; MnDOTA was measured at 86 K and 5 W. (d) Buildup of polarization for the DNP-enhanced signals under the same experimental conditions used for the enhancement measurements.

The dynamics of polarization buildup did not differ significantly among the three compounds investigated, as can be seen in Figure 5. The polarization buildup times are listed in Table 1 and are comparable to those using biradical polarizing agents.[17] The fact

dx.doi.org/10.1021/ja1109002 |J. Am. Chem. Soc. 2011, 133, 5648–5651

that deviations of the dynamics are negligible is not surprising. Generally, differences in the buildup times might be attributed to differences in the relaxation times of the paramagnetic center and the nuclei and variations in effective sample concentrations, among other things, as well as the actual rate of polarization transfer from the electron spin to the surrounding nuclei and the subsequent spreading of the polarization to the bulk via $^1H-^1H$ spin diffusion. The fact that the buildup and relaxation properties are very similar for all three compounds furthermore supports our finding that the DNP performance is mostly influenced by the actual widths of the DNP transitions, which in turn are closely related to the EPR line widths.

We have shown that dynamic nuclear polarization via the solid effect is possible using high-spin transition-metal compounds as polarizing agents. When the EPR line width is narrow and there is no spectral dilution by strong hyperfine coupling to the metal nucleus, DNP performance comparable to that obtained with the well-established trityl radical can be achieved. However, when significant broadening of the central transition by second-order ZFS or strong hyperfine coupling to the metal nucleus is present, the enhancement is strongly compromised. The depletion of the enhancement is not caused by alteration of the actual DNP process but rather simply due to more selective excitation of electron spins participating in DNP. In this context, we suggest that the higher effective transition moment of the high-spin system in combination with reduced line broadening caused by second-order ZFS might lead to improved performance of these compounds even at higher fields (e.g., 9 T and above).

■ ASSOCIATED CONTENT

Supporting Information. Sample preparation and experimental and instrumental details. This material is available free of charge via the Internet at http://pubs.acs.org.

■ AUTHOR INFORMATION

Corresponding Author
rgg@mit.edu

■ ACKNOWLEDGMENT

This research was supported by the National Institutes of Health through Grants EB002804 and EB002026. B.C. was partially funded by the Deutsche Forschungsgemeinschaft (Research Fellowship CO 802/1-1). A.B.B. was partially supported by an NSF Graduate Research Fellowship.

■ REFERENCES

(1) Bennett, A. E.; Ok, J. H.; Griffin, R. G.; Vega, S. *J. Chem. Phys.* **1992**, *96*, 8624.
(2) Bennett, A. E.; Rienstra, C. M.; Griffiths, J. M.; Zhen, W. G.; Lansbury, P. T.; Griffin, R. G. *J. Chem. Phys.* **1998**, *108*, 9463.
(3) Griffin, R. G. *Nat. Struct. Biol.* **1998**, *5*, 508.
(4) Jaroniec, C. P.; Filip, C.; Griffin, R. G. *J. Am. Chem. Soc.* **2002**, *124*, 10728.
(5) Rosay, M.; Tometich, L.; Pawsey, S.; Bader, R.; Schauwecker, R.; Blank, M.; Borchard, P. M.; Cauffman, S. R.; Felch, K. L.; Weber, R. T.; Temkin, R. J.; Griffin, R. G.; Maas, W. E. *Phys. Chem. Chem. Phys.* **2010**, *12*, 5850.
(6) Rosay, M.; Weis, V.; Kreischer, K. E.; Temkin, R. J.; Griffin, R. G. *J. Am. Chem. Soc.* **2002**, *124*, 3214.
(7) Rosay, M. M. Ph.D. Thesis, Massachusetts Institute of Technology, Cambridge, MA, 2001.
(8) Becerra, L. R.; Gerfen, G. J.; Temkin, R. J.; Singel, D. J.; Griffin, R. G. *Phys. Rev. Lett.* **1993**, *71*, 3561.
(9) Gerfen, G. J.; Becerra, L. R.; Hall, D. A.; Griffin, R. G.; Temkin, R. J.; Singel, D. J. *J. Chem. Phys.* **1995**, *102*, 9494.
(10) Hall, D. A.; Maus, D. C.; Gerfen, G. J.; Inati, S. J.; Becerra, L. R.; Dahlquist, F. W.; Griffin, R. G. *Science* **1997**, *276*, 930.
(11) Mak-Jurkauskas, M. L.; Bajaj, V. S.; Hornstein, M. K.; Belenky, M.; Griffin, R. G.; Herzfeld, J. *Proc. Natl. Acad. Sci. U.S.A.* **2008**, *105*, 883.
(12) Bajaj, V. S.; Mak-Jurkauskas, M. L.; Belenky, M.; Herzfeld, J.; Griffin, R. G. *Proc. Natl. Acad. Sci. U.S.A.* **2009**, *106*, 9244.
(13) van der Wel, P. C. A.; Hu, K. N.; Lewandowski, J.; Griffin, R. G. *J. Am. Chem. Soc.* **2006**, *128*, 10840.
(14) Debelouchina, G. T.; Bayro, M. J.; van der Wel, P. C. A.; Caporini, M. A.; Barnes, A. B.; Rosay, M.; Maas, W. E.; Griffin, R. G. *Phys. Chem. Chem. Phys.* **2010**, *12*, 5911.
(15) Debelouchina, G. T.; Platt, G. W.; Bayro, M. J.; Radford, S. E.; Griffin, R. G. *J. Am. Chem. Soc.* **2010**, *132*, 10414.
(16) Bayro, M. J.; Maly, T.; Birkett, N. R.; MacPhee, C. E.; Dobson, C. M.; Griffin, R. G. *Biochemistry* **2010**, *49*, 7474.
(17) Barnes, A. B.; Corzilius, B.; Mak-Jurkauskas, M. L.; Andreas, L. B.; Bajaj, V. S.; Matsuki, Y.; Belenky, M. L.; Lugtenburg, J.; Sirigiri, J. R.; Temkin, R. J.; Herzfeld, J.; Griffin, R. G. *Phys. Chem. Chem. Phys.* **2010**, *12*, 5861.
(18) Hu, K.-N.; Bajaj, V. S.; Rosay, M. M.; Griffin, R. G. *J. Chem. Phys.* **2007**, *126*, No. 044512.
(19) Hu, K.-N.; Song, C.; Yu, H.-h.; Swager, T. M.; Griffin, R. G. *J. Chem. Phys.* **2008**, *128*, No. 052321.
(20) Hu, K. N.; Yu, H. H.; Swager, T. M.; Griffin, R. G. *J. Am. Chem. Soc.* **2004**, *126*, 10844.
(21) Benmelouka, M.; Van Tol, J.; Borel, A.; Port, M.; Helm, L.; Brunel, L. C.; Merbach, A. E. *J. Am. Chem. Soc.* **2006**, *128*, 7807.
(22) Abragam, A.; Goldman, M. *Rep. Prog. Phys.* **1978**, *41*, 395.
(23) Goldman, M. *Spin Temperature and Nuclear Magnetic Resonance in Solids*; Oxford University Press: London, 1970.
(24) Barnes, A. B.; De Paepe, G.; van der Wel, P. C. A.; Hu, K. N.; Joo, C. G.; Bajaj, V. S.; Mak-Jurkauskas, M. L.; Sirigiri, J. R.; Herzfeld, J.; Temkin, R. J.; Griffin, R. G. *Appl. Magn. Reson.* **2008**, *34*, 237.
(25) Maly, T.; Debelouchina, G. T.; Bajaj, V. S.; Hu, K.-N.; Joo, C.-G.; Mak-Jurkauskas, M. L.; Sirigiri, J. R.; van der Wel, P. C. A.; Herzfeld, J.; Temkin, R. J.; Griffin, R. G. *J. Chem. Phys.* **2008**, *128*, No. 052211.
(26) Smith, A. A.; Corzilius, B.; Barnes, A. B.; Maly, T.; Griffin, R. G. In preparation.
(27) Abragam, A. *Principles of Nuclear Magnetic Resonance*; Oxford University Press: New York, 1961.
(28) Hu, K.-N.; Bajaj, V. S.; Rosay, M.; Griffin, R. G. *J. Chem. Phys.* **2007**, *126*, No. 044512.
(29) Becerra, L. R.; Gerfen, G. J.; Bellew, B. F.; Bryant, J. A.; Hall, D. A.; Inati, S. J.; Weber, R. T.; Un, S.; Prisner, T. F.; McDermott, A. E.; Fishbein, K. W.; Kreischer, K. E.; Temkin, R. J.; Singel, D. J.; Griffin, R. G. *J. Magn. Reson., Ser. A* **1995**, *117*, 28.
(30) Joye, C. D.; Griffin, R. G.; Hornstein, M. K.; Hu, K. N.; Kreischer, K. E.; Rosay, M.; Shapiro, M. A.; Sirigiri, J. R.; Temkin, R. J.; Woskov, P. P. *IEEE Trans. Plasma Sci.* **2006**, *34*, 518.
(31) Bajaj, V. S.; Hornstein, M. K.; Kreischer, K. E.; Sirigiri, J. R.; Woskov, P. P.; Mak-Jurkauskas, M. L.; Herzfeld, J.; Temkin, R. J.; Griffin, R. G. *J. Magn. Reson.* **2007**, *189*, 251.
(32) Nagarajan, V.; Hovav, Y.; Feintuch, A.; Vega, S.; Goldfarb, D. *J. Chem. Phys.* **2010**, *132*, No. 214504.
(33) Astashkin, A. V.; Schweiger, A. *Chem. Phys. Lett.* **1990**, *174*, 595–602.